
Proceedings of the Sixth International Conference on
Railway Technology: Research, Development and Maintenance
Edited by: J. Pombo
Civil-Comp Conferences, Volume 7, Paper 6.16
Civil-Comp Press, Edinburgh, United Kingdom, 2024
ISSN: 2753-3239, doi: 10.4203/ccc.7.6.16


# Validation of a movable-point turnout design: a complete vehicle-turnout interaction model

**C. Somaschini, Q. Li, S. Alfi, E. Di Gialleonardo and A. Collina**

**Department of Mechanical Engineering**
**Politecnico di Milano**
**Italy**

## Abstract

Railway turnouts are crucial elements of railway networks. They are subjected to severe dynamic interactions due to rapid variations in wheel-rail contact, leading to high dynamic forces and potential damage mechanisms such as wear, plastic deformation, and rolling contact fatigue. Therefore, the design of these components must account for high-frequency train-track interactions. This study validates the design of a high-speed turnout with a movable point rail by analysing the dynamic responses and estimating the maximum stresses of critical components considering different trains and different running conditions. A three-step numerical approach is used to simplify the three-dimensional critical components with complex shapes, simulate the dynamic interaction using a FE-multibody simplified system and calculate the stresses on critical components. This procedure also considers non-linear large-scale kinematic constraints. The results, compared to experimental data, show good agreements in terms of displacements, accelerations, and stresses, demonstrating that this multi-stage approach effectively estimates the most stressed elements and areas of a turnout, providing predictive insights into turnout behaviour under varying operational conditions.

**Keywords:** turnout, switches and crossings, railroad track, vehicle-track interaction, finite element method, multi-body dynamic simulation

# 1 Introduction

Turnouts (switches and crossings) are critical elements of railway network. The rapid varying wheel-rail contact geometry in different panels leads to severe train-track dynamic interaction and therefore high dynamic contact forces [1]. Wear, accumulated plastic deformation, and rolling contact fatigue (RCF) are common damage mechanisms in turnouts [2-4]. Consequently, the design of the critical components of a railway turnout should take account of the high frequency dynamics of train-track interaction generating high loads. However, the numerical simulation of the passage of a rolling stock over a turnout is a complex task and requires sophisticated mathematical models at different levels [5-8]. In the recent years, the interest on the topic from the academic community is continuously increasing as demonstrated by the benchmark [9].

The current study aims to validate the design of a high-speed-line turnout with a movable point rail (Figure 1) by analysing the dynamic responses of the critical components during train passages and estimating the maximum stresses of the same components, considering different types of trains at their maximum operating speed. A three-step numerical approach is used to simulate the train passage in both main and diverging directions. For all the steps FE (finite element) track models are adopted.

In the first step, the critical components of the switch (saddle, pointing rail, splice rail) are modelled as 3D solid parts in a detailed FE model to study their static and dynamic generalised behaviour.

In the second step, all the components of the turnout are modelled by 3D beam elements (rails, frog, sleepers), elastic elements (rail fastenings), and concentrated masses (mass of ballast) with the aim of reproducing the dynamic behaviour of the switch as the train passes. The main results of this step are time histories of the dynamic contact forces given by FE-Multibody simulations. It is worth noting that the non-linear large-scale motions of the components are also taken into account.

In the third step, a hybrid track model is used: rails and sleepers are simplified as for step two while critical components (frog, point rail, splice rail) are modelled as 3D solid parts to calculate the state of stress by applying the contact forces calculated in the previous step.

Finally, the numerical results are compared to some corresponding experimental data in terms of displacements, accelerations, and stresses of the main elements.

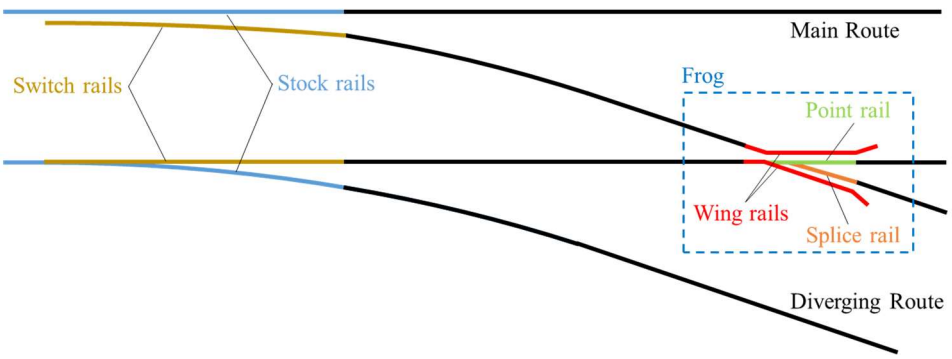


Figure 1: simplified scheme of the railroad switch with its main components.

## 2 Methods

In this section, more details of the three-step numerical approach introduced in the preceding section are given.

Regarding the first step, whose aim is to develop the 3D FE models of the main turnout components, the model of the frog is presented in Figure 2 (left) as an example (in the shape of its first eigenmode). The eigen parameters and quasi-static behaviour of the modelled components are studied and are used in the subsequent step of the approach, where the simplified FE models of the turnout components are developed. Specifically, the simplified FE models are composed of beam elements and lumped masses only, whose properties, such as the beam section properties, density, length, etc., are determined by fitting the first eigenfrequencies and mode shapes and the quasi-static behaviour of the 3D model. The simplified model of the frog is shown in Figure 2 (right) in the shape of its first eigenmode, which is highly similar to that of the 3D model.

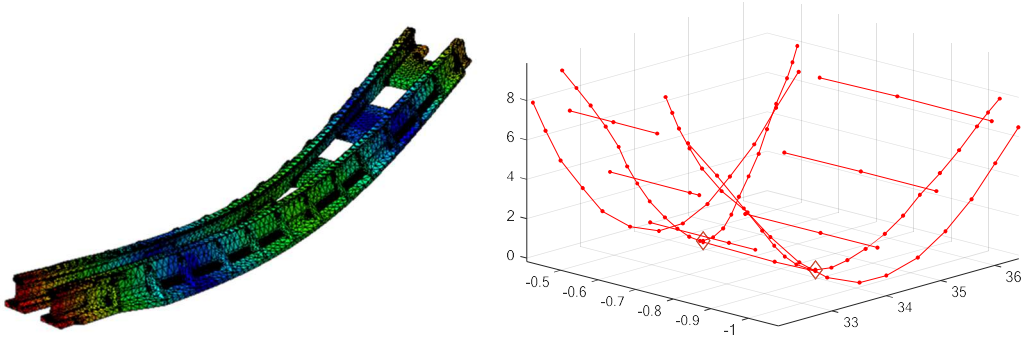


Figure 2: Comparison of the first bending mode of the frog: 3D solid FE model (left) and simplified FE model (right).

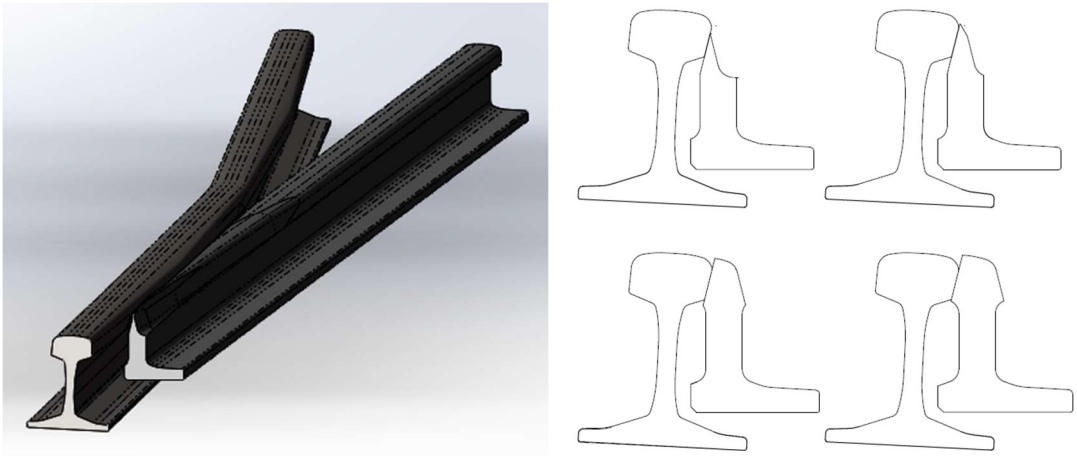

Figure 3: Examples of section variations along the switch rail.

Within the second step of the approach, the simplified turnout model is used by the program ADTreS [1], a train-track dynamic interaction simulation environment. In this simulation environment, the train and track are regarded as two individual subsystems and dynamically coupled through contact forces. In other words, the equations of motion of the two subsystems are derived separately, and are numerically integrated simultaneously in time domain together with the contact forces. The train model is obtained using a multi-body approach while the turnout is modelled by means of a FE approach, and all the components of the turnout are modelled by 3D beam elements (rails, saddle, sleepers), elastic elements (rail fastenings), and concentrated masses (mass of ballast). The elements of each subsystem are connected by elastic and damping elements and, eventually, by nonlinear force elements.

Differently from the case of a train running on a tangent track, the analysis of a railway switch has to carefully and properly deal with several complications for the modelling and simulation. The most important concerns to be addressed are the multi-point wheel-rail contact and the varying geometry along the switch rail (Figure 3) and point rail, which leads to a continuously changing contact condition. Furthermore, these two issues overlap on the passage of the contact point between different rails, for instance from the stock rail to the switch rail and from the wing rail to the point rail.

As for the connections between the components, it is fundamental to develop the unilateral contact between some components, such as between the stock and switch rail or the point and wing rail, as constrained by the physical contacts.

The simulation results of this step include the time history of the contact forces and the displacements of various components of the turnout. Subsequently, the dynamic forces acting on the beam elements and the corresponding state of stress can be directly calculated by the displacement. However, the calculation of state of stress considering beam elements is valid only for some components of the turnout (e.g. stock rail, switch rail) but not for components with more complex geometry (e.g. saddle, point rail).

To study the stresses on the elements with complex geometry, the third step is needed. The FE model in this case is a combination of the previous ones, i.e., the substructure of rails and sleepers is simplified with beams and concentrated elements while the critical components with complex geometry are modelled as 3D solid parts (Figure 4).

The force applied on the hybrid model and the corresponding contact points are those computed in the previous step with the simplified models, and the stress evolution in time of the most critical points during the entire passage of the train are computed.

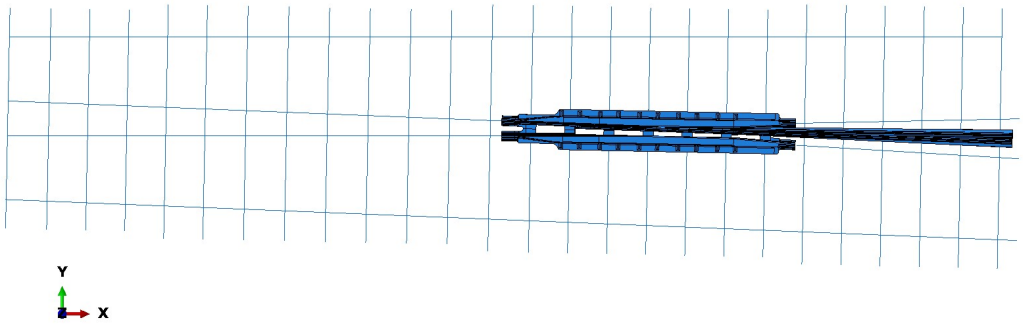


Figure 4: finite element model of the closure and crossing panels of the studied turnout, employed in the second-step simulation with program Abaqus, constituted by beam element, concentrated mass and 3D solid parts (saddle, point rail and splice rail).

## 3 Results

Examples of the numerical results are presented hereinafter. All the results refer to the study case of a passage of a high-speed train ETR500 at 300 km/h on the main line direction (i.e. the point rail is in contact with saddle on the right hand side), and some of them are compared to experimental data.
Considering the simplifications of the different models, all the results are filtered using a low-pass filter with a cutoff frequency of 100 Hz.

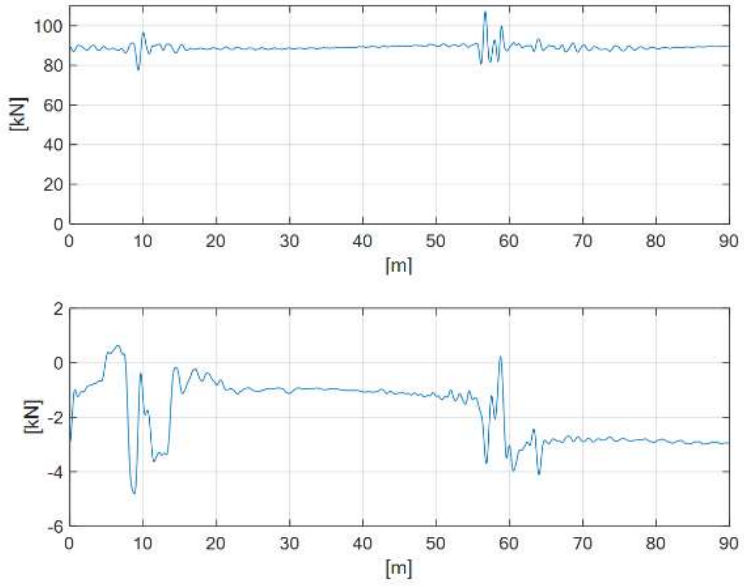


Figure 5: simulated time history of contact forces acting on the wheel of the first wheelset during the complete passage of the turnout (ETR 500 at 300 km/h in the main line direction): vertical force (upper), lateral force (lower).

Concerning the second step of the simulation, the vertical component of the contact force acting on the wheel of the leading wheelset during the complete passage of the turnout is presented in Figure 5.
These results help to understand whether the passage of the train, albeit under conditions of theoretical rectilinear motion, imposes strong dynamic forces on the turnout. The clearly visible perturbations in the time history of the vertical contact force (upper plot of the Figure 5) and of the lateral contact force (lower plot of the Figure 5) around 10 m and 60 m are related to the passage of the wheel over the switch toe and the crossing nose (swing nose).
From the second step of simulation, it is also possible to directly extract the strains and the stresses of the rails. By way of example, Figure 6 (on the left) shows the axial strains of the switch rail foot during the passage of a coach. The results are shown on a space-time diagram for 24 sections along the rail since it was possible to validate these results by means of experimental measurements obtained by means of with fibre-optic strain gauges (righthand side of Figure 6). From the comparison of Figure 6 it is possible to see that the experimental and simulated results share a high similarity both in terms of the temporal and spatial trend and in terms of absolute level of the deformation.
Observing the space-time evolution of Figure 6, it can be observed that the strain gradually increases along the switch rail since the loads transfer from the stock rail to the switch rail. Afterwards, once the loads has completely transferred onto the switch rail, the strain decreases s as the switch rail section increases.
Considering these opposite evolutions, the most stressed area is clearly visible between sections 7 and 10 where on the one hand the contact point between wheel and rail passes from the stock rail to the switch rail and, on the other hand, the rail cross-section is still rather reduced.

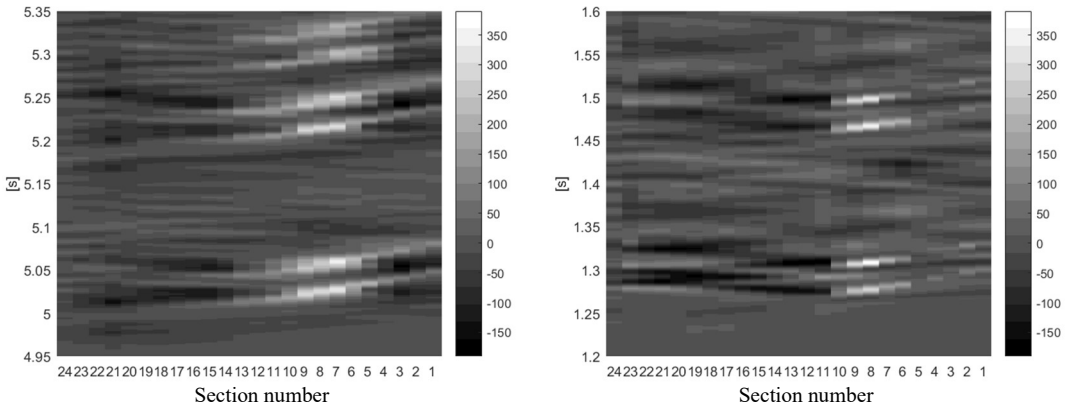


Figure 6: deformation of the switch rail (in με) in the main line direction in the case of train ETR500 at 330 km/h: experimental (left) and simulated (right).

Considering the third step, the stresses of the saddle, evaluated at the bottom external edges and represented by von-Mises criterion, are reported in Figure 7.
The results show that the stress on the bottom edge of the right-hand side of the saddle (in contact with the point rail for the main line direction) is much higher than the one

of the left-hand side while the most stressed point was found to be on the inner edge under the point rail.

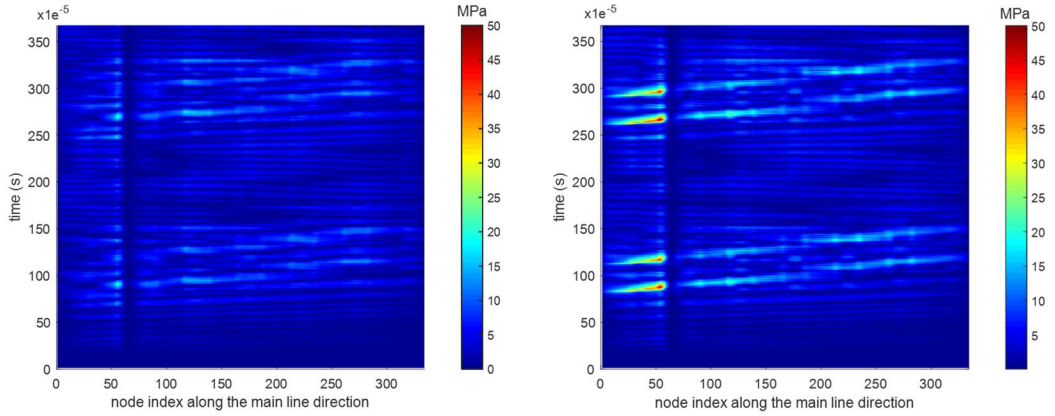


Figure 7: simulated time history of von-Mises stress of the saddle during the passage of a high-speed train coach (ETR 500 at 300 km/h in the main line direction): external bottom edge on the left hand side (left), external bottom edge on the right hand side (right).

# 4 Conclusions and Contributions

The current study aims to analyse a high-speed line turnout with a movable point rail subjected to train-track dynamic interactions in terms of the dynamic behaviour and the state of stress of the crucial components. A three-step numerical simulation approach is proposed.

In the first step, a 3D FE model of the most complex elements is used as a reference for a simplification to beam elements.

The second step employs a multi-body model of the train coupled with the simplified FE track model constituted by beams and concentred elements to obtain the dynamic contact forces.

The third step substituted the crucial components with 3D solid parts and their state of stress is calculated considering the forces evaluated in the previous step.

The numerical simulation of the rail-wheel contact problem takes account of the multiple contact points on different components and the consequent load transfer, the varying rail geometry, the deformability of all track components and the nonlinear unilateral contact between different track components.

The simulation results allow to obtain time-space evolution of the dynamic contact force generated by the train-turnout interaction and the time history of the deformation and state of stress of different components.

The comparison between the numerical results with experimental data in terms of the deformation and displacements of some key elements of the switch rail shows that the model used, albeit simplified, is able to reproduce the dynamics of the passage of a train. The calculated stress values are aligned with those measured trackside in terms both of time evolution and both of maximum values.

This type of multi-stage model therefore makes it possible to estimate the most stressed elements and areas of a turnout in service, as well as to predict its behaviour, e.g. by increasing speed or train axle loads.

# References


[1] S. Alfi & S. Bruni (2009) Mathematical modelling of train–turnout interaction, Vehicle System Dynamics, 47:5, 551-574.

[2] B.A. Pålsson, J.C.O. Nielsen (2012), Wheel–rail interaction and damage in switches and crossings, Vehicle System Dynamics, 50:1, 43–58.

[3] E.J.M. Hiensch, N. Burgelman (2017) Switch Panel wear loading–a parametric study regarding governing train operational factors, Vehicle System Dynamics, 55:9, 1384–1404.

[4] E. Kassa, G. Johansson (2007) Simulation of train-turnout interaction and plastic deformation of rail profiles, Vehicle System Dynamics, 44:SUPPL. 1, 349–359

[5] B.A. Pålsson, J.C.O. Nielsen (2015) Dynamic vehicle–track interaction in switches and crossings and the influence of rail pad stiffness – field measurements and validation of a simulation model, Vehicle System Dynamics, 53:6, 734-755.

[6] H. Vilhelmson, B.A. Pålsson, J.C.O. Nielsen, U. Ossberger, M. Sehner, H. Loy, (2024) Dynamic vehicle–track interaction and structural loading in a crossing panel – calibration and assessment of a model with a 3D representation of the crossing rail, Vehicle System Dynamics, 1–23.

[7] B.A. Pålsson, H. Vilhelmson, U. Ossberger, M. Sehner, M.D.G. Milosevic, H. Loy, J.C.O. Nielsen (2024) Dynamic vehicle–track interaction and loading in a railway crossing panel – calibration of a structural track model to comprehensive field measurements. Vehicle System Dynamics, 1–27.

[8] H. Magalhaes, F. Marques, P. Antunes, P. Flores, J. Pombo, J. Ambrósio, A. Qazi, M. Sebes, H. Yin, Y. Bezin (2022) Wheel-rail contact models in the presence of switches and crossings. Vehicle System Dynamics, 61:3, 838–870.

[9] B.A. Pålsson, Y. Bezin, (2023). Editorial for S&C benchmark special issue. Vehicle System Dynamics, 61:3, 639–643.